A Cascade of Structure in a Drop Falling from a Faucet

X. D. Shi, Michael P. Brenner, Sidney R. Nagel

A drop falling from a faucet is a common example of a mass fissioning into two or more pieces. The shape of the liquid in this situation has been investigated by both experiment and computer simulation. As the viscosity of the liquid is varied, the shape of the drop changes dramatically. Near the point of breakup, viscous drops develop long necks that then spawn a series of smaller necks with ever thinner diameters. Simulations indicate that this repeated formation of necks can proceed ad infinitum whenever a small but finite amount of noise is present in the experiment. In this situation, the dynamical singularity occurring when a drop fissions is characterized by a rough interface.

What happens when liquid drips from a faucet? As it falls, its topology changes from a single mass of fluid into two or more drops. This common phenomenon is one of the simplest hydrodynamic examples of a singularity (*1*) in which physical quantities become discontinuous in a finite time. Here, we investigate the shape of this singularity for fluids of varying viscosity dripping through air from a cylindrical nozzle. Scientific studies of this system date back to Lord Rayleigh's stability analysis of a liquid cylinder (*2*) and Plateau's analysis of a hanging pendant droplet (*3*). More recent work has begun to address the shape of the interface near the singularity. Eggers and Dupont (*4*) simulated falling droplets by means of the Navier-Stokes equations and showed that their solutions agreed with the experimental shapes of water photographed by Peregrine *et al.* (*5*).

Although our study focuses on a specific experimental system, the dynamics near a singularity should be insensitive to changes in the initial conditions and external forcing within a wide range of parameters. Thus, the shape of the interface near the breakup point should not depend on whether the drop is falling in a gravitational field or being pulled apart by shear forces (*6*). This expectation arises from the realization that as the interface breaks, its thickness must eventually become much smaller than any other length in the problem (until microscopic atomic scales are reached). In this regime, the only length (*7*) that can affect the dynamics is the thickness of the fluid itself, so that the simplest assumption for the dynamics is self-similarity—that is, the shape near the singularity changes in time only by a change in scale. The mathematical definition of a similarity solution is

$$h(z,t) = f(t)H\left[\frac{z - z_0}{f(t)^\beta}\right] \qquad (1)$$

where h describes the radius of the drop as a function of the vertical coordinate z and time t; $f(t)$ is an arbitrary function of time; β is a constant; and z_0 is the position where the droplet breaks. This scaling hypothesis has worked well in describing other types of singularities, ranging from critical phenomena (*8*) to droplet breakup in a two-dimensional Hele-Shaw cell (*9*, *10*). Also, for our problem here Eggers (*11*) constructed a similarity solution that showed good agreement with numerical solutions to the Navier-Stokes equation at low viscosities. On the other hand, Pumir, Siggia, and co-workers (*12*) have analyzed several mathematical models of singularities with a high Reynolds number that showed nonsteady corrections to Eq. 1. However, to the best of our knowledge those models did not have an experimental realization. For the case of the dripping faucet, we will show that both views have some validity: the similarity solution provides a basis for the underlying structure, but there are time-dependent corrections to this solution that alter the shape dramatically.

There are three independent length scales that characterize the hydrodynamics of the dripping faucet (*4*): (i) the diameter of the nozzle D; (ii) the capillary length

$$L_\gamma = \left(\frac{\gamma}{\rho g}\right)^{1/2}$$

which gives the balance between surface tension, γ, and the gravitational force ρg, where ρ is the fluid density and g is the acceleration of gravity; and (iii) the viscous length scale

$$L_\eta = \frac{\eta^2}{\rho\gamma}$$

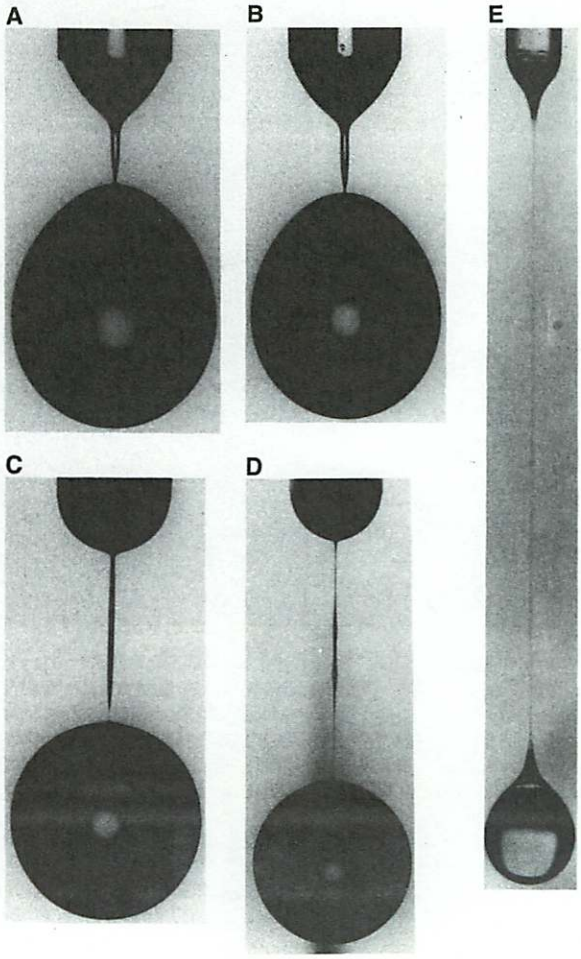

Fig. 1. The shape close to the time of breakup of five drops with different viscosities. The liquids, with $\eta = 10^{-2}$ P (**A**), 10^{-1} P (**B**), 1 P (**C**), 2 P (**D**), and 12 P (**E**), were allowed to drain slowly through a glass tube with a nozzle diameter D of 1.5 mm. (A) and (E) show pure water and pure glycerol, respectively. We used an 80-mm Hasselblad lens attached to a bellows and a still camera; the drop was illuminated from behind by a fast (≈5 μs) flash from a strobe (EG&G model MVS 2601, Salem, Massachusetts) that was triggered with a variable delay from the time the drop intersected a laser beam incident on a photodiode.

James Franck Institute and Department of Physics, University of Chicago, 5640 South Ellis Avenue, Chicago, IL 60637, USA.

where η is the viscosity. For water (*5*), $L_\eta \approx 100$ Å. For that system, it is not possible to photograph the shape of the interface where the thickness is asymptotically smaller than L_η because current optical techniques cannot resolve objects much smaller than 1 μm.

To find the asymptotic shape of the singularity, we studied droplet snap-off as a function of viscosity. By mixing glycerol into water, we can increase the viscosity by a factor of 10^3 so that L_η can be increased by 10^6 while the surface tension is not varied by more than 15% (*13*). We thoroughly mixed the water and glycerol, taking care to eliminate air bubbles. The shapes close to the breakup point of five liquids with different viscosities draining slowly from a nozzle of diameter $D = 1.5$ mm vary as the viscosity is varied (*14*) (Fig. 1). As the value of η increases, the neck of the drop elongates and forms structures not observable in dripping water. Herein, we concentrate our attention on the structure of a drop of liquid with intermediate viscosity and report a combination of photographic studies of the singularity and numerical simulations of the Navier-Stokes equations.

As a drop of an 85% glycerol and 15% water mixture [$\eta = 1$ poise (P), where 1 P = 1 dyne·s cm^{-2}, and $L_\eta = 0.13$ mm] breaks (Fig. 2), it forms a long thin neck of fluid connecting the nozzle exit plane (a flat brass plate) to the main part of the drop. A closeup photograph (Fig. 2B) gives a clearer view of the region just above the main drop where the neck decreases in width, forming a secondary neck. At a slightly later time (Fig. 2C), this secondary neck suffers an instability and forms a third neck. We estimate the thickness of the smallest neck in Fig. 2C to be about 5 μm. Through high-speed photography, we have verified that both the second neck and the third neck develop by a similar process: an initial thinning near the drop is followed by a rapid extension of the neck upward away from the drop. This leads us to suspect that the repeated formation of such necks could happen indefinitely. Our simulations described below can produce such a phenomenon ad infinitum (with as many as seven successive necks at the resolution limit) as long as a noise source is present. On the other hand, in the absence of noise, our simulations indicate that near the singularity the interface is smooth. We argue that noise, which is always present in the experiment, invariably leads to a singularity with complex structure.

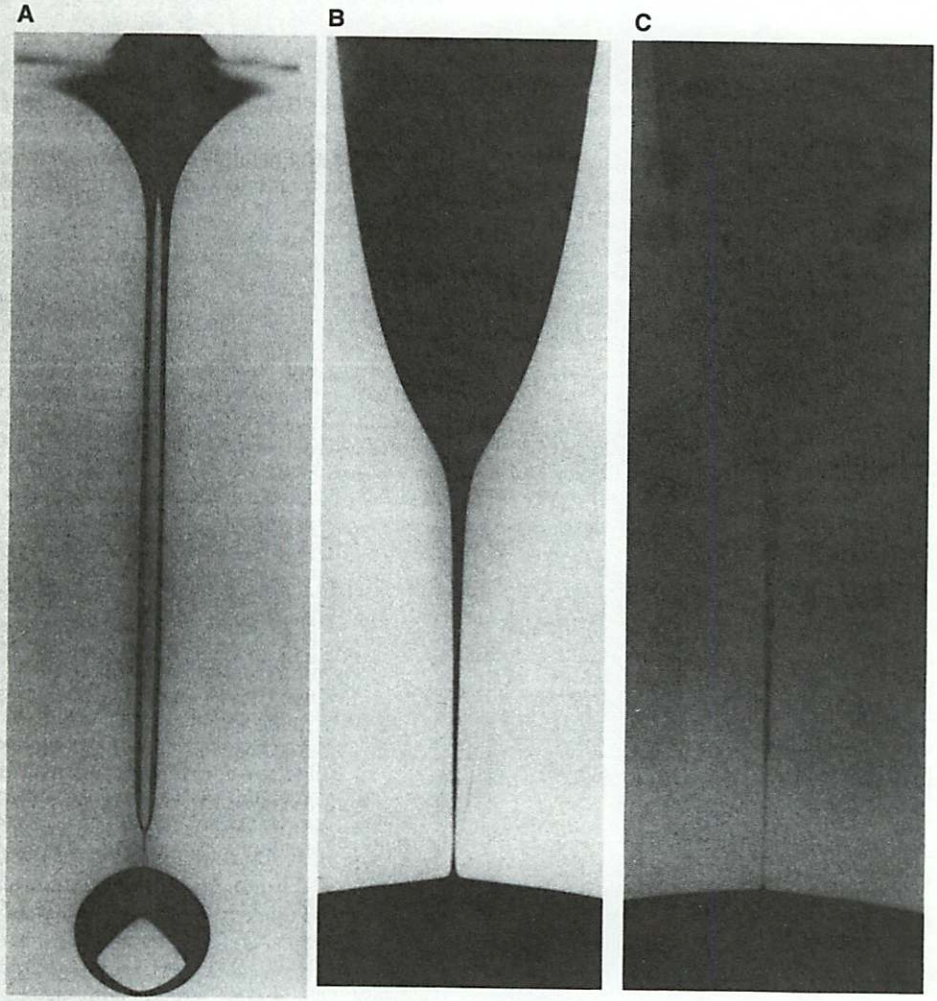

Fig. 2. A photograph of a drop of a glycerol in water mixture (85 weight %). (**A**) The initial stages of the breakup as the droplet separates from the nozzle by a long neck. A secondary neck is visible just above the main drop. (**B**) A magnified view of the region near the breakup point (obtained from a different photograph). The thickest region in this picture corresponds to the long neck of (A). Only one secondary neck is visible. (**C**) The same region as in (B) but at a slightly later time. The second neck and a well-developed third neck are clearly visible in this picture. Using the Eggers similarity solution, we estimate that (B) and (C) are 2×10^{-3} and 2×10^{-4} s, respectively, before the time of breakup. The photographs were taken as in Fig. 1, except with a 35-mm lens. Because the clearest demonstration of the structure of the singularity was obtained with the use of the largest drop, we found it advantageous to replace the glass nozzle by a brass plate riddled with numerous small holes on which the liquid would slowly collect before falling. The diameter of the drop at the plate was approximately 20 mm.

Numerical simulations of the Navier-Stokes equations have provided a well-developed tool for reproducing the large-scale structures and velocities of fluid flows. In addition, they can investigate structure on finer scales than can be seen in the figures here. Our simulations used the equations of Eggers and Dupont (*4*), which are approximate versions of the Navier-Stokes equations (for a Newtonian fluid) that neglect non-axisymmetric effects (*4*, *15*, *16*):

$$\rho\left(\frac{\partial v}{\partial t} + v\frac{\partial v}{\partial z}\right) = \frac{3\eta}{h^2}\frac{\partial}{\partial z}\left(h^2\frac{\partial v}{\partial z}\right) - \frac{dp}{dz} + \rho g \quad (2)$$

$$\frac{\partial h^2}{\partial t} + \frac{\partial (h^2 v)}{\partial z} = 0 \quad (3)$$

$$p = \frac{\gamma}{h}\left[1 + \left(\frac{\partial h}{\partial z}\right)^2\right]^{-1/2} - \gamma\left[1 + \left(\frac{\partial h}{\partial z}\right)^2\right]^{-3/2}\frac{\partial^2 h}{\partial z^2} \quad (4)$$

where $h(z)$ is the radius of the fluid neck a distance z from the nozzle, and $v(z)$ is the fluid velocity. Equation 2 expresses force balance: the acceleration is due to viscous stresses, a pressure gradient, and gravity; Eq. 3 expresses local mass conservation; and Eq. 4 specifies that the pressure jump across the interface is determined by its mean curvature. These equations were solved with a modified version of a finite-difference scheme supplied by Eggers and Dupont (*4*). An adaptive grid, similar to that of Bertozzi *et al.* (*17*), allowed high resolution of the singularity. At prescribed

time intervals, the grid was adjusted.

In Fig. 3, we present the results of numerical simulations for a liquid with a viscosity of 1 P falling from a nozzle with a diameter $D = 4.5$ mm. Figure 3A shows the drop profile approximately 10^{-8} s before rupture. The shape of the interface near the drop is similar to that shown in Fig. 2A (*18*). In a magnification of the region of the secondary neck (Fig. 3B), the interface thins near the main drop. This thinning continues smoothly to arbitrarily small scales. Near the singularity, the interfacial shape is well approximated by the similarity solution proposed by Eggers and first seen by Eggers and Dupont (*4*). However, these simulations show no evidence of the repeated formation of necks, as shown in Fig. 2.

To induce the repeated formation of such necks in the simulations, it was necessary to introduce a noise source explicitly. We did this by placing fluctuations, on the order of 10^{-4} the minimum thickness of the neck, on the interface during the simulation. Both the temporal and spatial separation between subsequent fluctuations were small compared to the characteristic scales of the Eggers similarity solution. Our results (10^{-8} s before break-off) show a magnification of the secondary neck (Fig. 4A) and the highest resolution attainable with our present code (Fig. 4B). The smallest neck shown in Fig. 4 is only 2 Å wide. At each level, before a new neck starts to form, the shape of the interface was approximated by the similarity solution of Eggers. This result demonstrates that, at the point of breaking, fission proceeds by means of the formation of necks that themselves form necks down to the smallest level detectable.

Noise fluctuations in the shape of the interface become more effective at creating additional structures as the thickness of the interface decreases (*19*). The amount of noise introduced in the simulations above corresponds to angstrom-size fluctuations of the interface when the thickness of a neck is still on the order of 1 μm. Thus, even thermal fluctuations may be sufficient to produce these effects. The only caveat is that because this is a strongly nonequilibrium situation, we do not understand the spectrum of the noise in the experiment. However, there are many sources of noise, ranging from surfactants on the interface, to pressure fluctuations in the nozzle, to air currents in the room, shear heating in the liquid, and thermal fluctuations (for example, excitation of capillary waves). In our experiment, we might also expect noise generated from fluctuations in the concentration of the two liquids as well as from evaporation from the surface. On repeating the experiment, we found that the details of the interfacial shape can vary: the precise position of the necks can change from drop to drop and blobs can form on the interface at irregular intervals. Nevertheless, the repeated formation of necks appears to be robust. (Our simulations with a noise source also produce such variations when different realizations of the noise are used.)

Taken together, our results show that the singularity in the fission of a drop is characterized by the repeated formation of necks, which may proceed ad infinitum in the presence of a small noise source. The shape of the interface near this singularity is therefore rough, with a time-dependent structure in contrast to the scaling hypothesis of Eq. 1 (*20*). The description of this singularity is more complicated, with new structures evolving progressively more frequently in time (*21*). In a real fluid, such repeated formation of necks can occur only a finite number of times. Once the neck becomes thin enough, a hydrodynamic description breaks down as long-range van der Waals forces and molecular effects become important. In this regime, simulators have used molecular dynamics techniques (*22, 23*) to study such a breakup.

In our experiments, after the drop detached from the bottom of the neck a satellite droplet formed from the long neck itself and separated from the fluid near the nozzle. The singularity in this case had a structure similar to the one described above (where the drop separated from the bottom of the neck), and in both cases the thinnest necks were attached to a large, almost spherical mass of fluid. However, for the upper singularity, the diameters of the necks increased with distance from the nozzle (in the direction of gravity), which is opposite to what happens in the situation at the bottom of the neck where the diameters decreased (against the direction of gravity). The form of the singularity thus appears to be invariant to the direction of the external forcing.

We have shown that the singularity found in the fission of a viscous drop of liquid is different from what had been expected from earlier observations of less viscous fluids. Instead of a smooth interface, we found (to the limit of our resolution) a rough interface with necks "growing" other necks. The existence of this phenomenon appears to depend on the presence of experimental noise. However, it should be pointed out that because our simulations used only an approximation of the Navier-Stokes equations, it is possible that such a cascade of necks could form by a deterministic mechanism in the full equations. Our results raise many questions: To what extent does the regular repetition of the formation of these necks depend on the characteristics of the noise source? Under what circumstances can the interfacial shapes develop even more structure? And what is the spectrum of noise in a typical experiment?

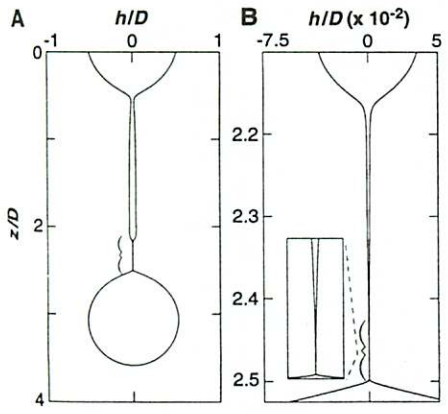

Fig. 3. Simulation of the profile for a drop of a glycerol in water mixture (85 weight %; viscosity = 1 P) falling from a nozzle of diameter $D = 4.5$ mm. (**A**) A view of the entire drop, at approximately 10^{-8} s before snap-off, shows that near the bottom of the long neck there is a region where the thickness decreases and forms a secondary neck. (**B**) An enlargement of the region in (A) enclosed by brackets. Note that the scales are different along the two axes, so that the shape can be easily seen. The inset shows another, greater magnification.

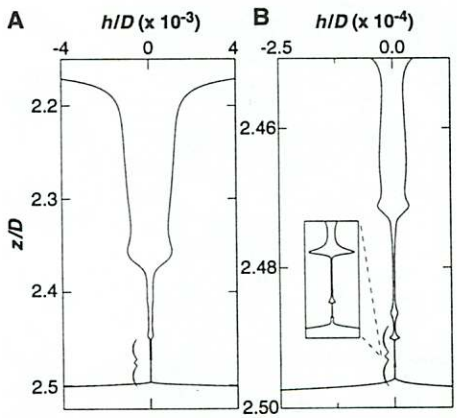

Fig. 4. Simulation of the same drop as in Fig. 3 in the presence of noise. A view of the entire drop is indistinguishable from that in Fig. 3A. (**A**) An enlargement of the first neck (as in Fig. 3B) shows a third, fourth, and (very thin) fifth neck sprouting from the second neck. (**B**) An enlargement of the bracketed region of (A) shows the fourth and fifth necks of the previous figure, as well as the sixth neck. In the inset, a magnification of the sixth neck shows a seventh neck.

REFERENCES AND NOTES

1. A. Pumir and E. D. Siggia, *Phys. Rev. Lett.* **68**, 1511 (1992).
2. W. S. Rayleigh, *Proc. London Math. Soc.* **4**, 10 (1878).
3. J. Plateau, *Statique Expérimentale et Théoretique des Liquides Soumis aux Seules Forces Moléculaires* (Gauthier-Villars, Paris, 1873).
4. J. Eggers and T. F. Dupont, *J. Fluid Mech.* **262**, 205 (1994).

5. D. H. Peregrine, G. Shoker, A. Symon, *ibid.* **212**, 25 (1990).
6. M. Tjahjadi, H. A. Stone, J. M. Ottino, *ibid.* **243**, 297 (1992).
7. We note that, nevertheless, the solution near the singularity must still be measured in terms of a length scale relevant to the dynamics in the problem. This scale is the viscous length defined below.
8. C. Domb and M. S. Green, Eds., *Phase Transitions and Critical Phenomena* (Academic Press, London, 1972).
9. P. Constantin *et al.*, *Phys. Rev. E* **47**, 4169 (1993).
10. R. E. Goldstein, A. I. Pesci, M. J. Shelley, *Phys. Rev. Lett.* **70**, 3043 (1993).
11. J. Eggers, *ibid.* **71**, 3458 (1993).
12. A. Pumir, B. I. Shraiman, E. D. Siggia, *Phys. Rev. A* **45**, R5351 (1992); T. Dombre, A. Pumir, E. D. Siggia, *Physica D* **57**, 311 (1992).
13. G. W. C. Kaye and T. H. Laby, *Tables of Physical and Chemical Constants* (Longman, New York, 1986); J. B. Segur and H. E. Oberstar, *Ind. Eng. Chem.* **43**, 2117 (1951).
14. E. A. Hauser, H. E. Edgerton, W. B. Tucker, *J. Phys. Chem.* **40**, 973 (1936); H. E. Edgerton, E. A. Hauser, W. B. Tucker, *ibid.* **41**, 1017 (1937).
15. Similar equations have been derived independently by S. E. Bechtel, J. Z. Cao, M. G. Forest [*J. Non-Newtonian Fluid Mech.* **41**, 201 (1992)] in the context of a general mathematical study of the dynamics of viscoelastic fluids. Their derivation includes Eqs. 2 and 3 as a special case, with a slightly different form for Eq. 4.
16. A similar equation (without the correct coefficient in front of the term with viscosity) was proposed by R. W. Sellens [*Atomization Sprays* **2**, 236 (1992)].
17. A. L. Bertozzi, M. P. Brenner, T. F. Dupont, L. P. Kadanoff, in *Centennial Edition, Applied Mathematics Series*, L. Sirovich, Ed. (Springer-Verlag Applied Mathematics Series, New York, 1993).
18. The boundary conditions used at the top of the drop in the simulation are different from those that actually apply in the experiment. We believe that this accounts for the differences in the two figures near the nozzle.
19. M. P. Brenner, X. D. Shi, S. R. Nagel, unpublished results.
20. From the Eggers similarity solution, one can show that the Reynolds number is ≈1. This situation is distinct from other models considered (*1*, *12*).
21. Tjahjadi *et al.* (*6*) observed a different hydrodynamic phenomenon that also had a fractal spatial structure. By allowing a stretched drop to relax, they found a sequence of droplets with sizes that decreased in a geometric progression. Our situation differs from theirs in that the repeated formation of necks is a property of the singularity itself and not the result of multiple breakup events.
22. J. Koplik and J. R. Banavar, *Phys. Fluids A* **5**, 521 (1993).
23. U. Landman, W. D. Luedtke, N. A. Burnham, R. J. Colton, *Science* **248**, 454 (1990).
24. We thank J. Eggers and T. Dupont for many helpful discussions and for generously sharing their numerical code and for showing us how to use it. We thank R. Leheny for initiating the experiments on the droplet breakup, R. Jeshion for help in the photographic development, O. Kapp for help in obtaining a fast camera, and E. Siggia for useful comments. D. Grier and D. Mueth helped us analyze the photographs digitally, and N. Lawrence made measurements of drop mass. We also thank A. Bertozzi for advice and L. Kadanoff for, among many other things, stimulating our interest in this subject. Supported by NSF grants DMR-MRL 88-19860 and DMR 91-11733, and Department of Energy grant DE-FG02-92ER25119.

1 February 1994; accepted 4 April 1994

Thermophysiology of *Tyrannosaurus rex*: Evidence from Oxygen Isotopes

Reese E. Barrick* and William J. Showers

The oxygen isotopic composition of vertebrate bone phosphate (δ_p) is related to ingested water and to the body temperature at which the bone forms. The δ_p is in equilibrium with the individual's body water, which is at a physiological steady state throughout the body. Therefore, intrabone temperature variation and the mean interbone temperature differences of well-preserved fossil vertebrates can be determined from the δ_p variation. Values of δ_p from a well-preserved *Tyrannosaurus rex* suggest that this species maintained homeothermy with less than 4°C of variability in body temperature. Maintenance of homeothermy implies a relatively high metabolic rate that is similar to that of endotherms.

Dinosaurs dominated the terrestrial landscape for 163 million years, from their origin in the mid-Triassic to their extinction at the end of the Cretaceous (*1*). Whether they were warm-blooded (tachymetabolic endotherms), cold-blooded (bradymetabolic ectotherms), or something in between (*2*) has been uncertain. A group as successful and diverse as the Dinosauria may have employed a wide range of thermal physiological strategies, some of which are not represented in extant terrestrial vertebrates.

Endothermy is a pattern of thermoregulation in which body temperature depends on a high and controlled rate of metabolic heat production (*3*). In ectothermy, body temperature is dependent on behaviorally and autonomically regulated uptake of heat from the environment. These patterns of thermoregulation are end members along a continuum of physiological strategies. In homeothermy, cyclic body temperature variation, either nyctohemerally or seasonally, is maintained within ±2°C despite much larger variations in ambient temperature (*3*). Large dinosaurs must have grown quickly to reach sexual maturity within an ecologically feasible length of time. The high metabolic rates of endotherms and the high efficiency of energy production of ectotherms are contrasting physiological strategies for solving this problem (*2*). Arguments for particular strategies of thermoregulation have been based on posture, bone histology, predator-prey relations, feeding mechanics, brain size, postulated behaviors, and paleobiogeography. Though innovative, these lines of evidence have ultimately proven to be inconclusive.

In this study, we used the oxygen isotopic composition of bone phosphate (δ_p) to calculate the body temperature variability of *Tyrannosaurus rex*. The phosphate-water isotopic temperature scale was developed for marine invertebrates (*4*) and later confirmed to be accurate for fish (*5*) and mammals (*6*). Vertebrate δ_p is a function of the body temperature at which bone forms and of the isotopic composition of body water (*7*, *8*). The isotopic composition of body water (δ_{bw}) depends on the $\delta^{18}O$ of water ingested during feeding and drinking as well as on the metabolic rate relative to water turnover rates (*8*, *9*). The body water of air-breathing vertebrates is at a physiological steady state but is not in equilibrium with environmental water. Several studies have demonstrated that δ_p is linearly offset from the $\delta^{18}O$ values of the local meteoric water, from the relative humidity, or from the ambient water (in the case of marine mammals) (*10*). Without knowledge of the $\delta^{18}O$ values (*11*) of body water for each fossil species, it is not possible to calculate actual body temperatures. However, all body water compartments in individual mammals have essentially identical $\delta^{18}O$ values (*12*). The variations in δ_p among skeletal elements in an individual should therefore reflect relative differences in body temperature. Temperature differences between the core body (the trunk) and the extremities can be calculated by use of the bone isotopic differences ($\Delta\delta_p$) and the slope of the phosphate-water paleotemperature equation (*4*, *5*).

An assessment of the isotopic integrity of the fossil bone material being examined is crucial for paleophysiological interpretations. We analyzed a *T. rex* specimen from the Maastrichtian Hell Creek Formation for δ_p and for the isotopic composition of both the structural bone carbonate (δ_c) and the coexisting calcite cements (δ_{cc}) (*13*). This specimen was chosen because of its excellent preservation (*14*). Two lines of evidence demonstrated that the bone phosphate analyzed was likely to reflect the original isotopic signal of growth. One test compared δ_p and the isotopic composition of structural carbonate (δ_c) with the isotopic composition of the diage-

Department of Marine, Earth, and Atmospheric Sciences, North Carolina State University, Raleigh, NC 27695–8208, USA.

*To whom correspondence should be addressed.